

On the reliability of attenuation measurements from ambient noise cross-correlations

Fan-Chi Lin, Michael H. Ritzwoller, & Weisen Shen

Center for Imaging the Earth's Interior, Department of Physics, University of Colorado at Boulder, Boulder, CO 80309-0390 USA (fan-chi.lin@colorado.edu)

We compare spatially averaged Rayleigh wave attenuation between 10 and 18 sec period observed on the symmetric component of ambient noise cross-correlations with regional seismic event measurements observed by the USArray Transportable Array across the western US. The ambient noise attenuation measurements are shown to be consistent with attenuation observed following an earthquake in Nevada and a mining blast in Wyoming. We further demonstrate that common ambient noise data processing procedures such as temporal normalization and spectral whitening can be retained as long as the amplitudes of the cross-correlations are corrected for (1) the duration of the ambient noise cross-correlation, (2) geometrical spreading, and (3) the azimuthal variation in the strength of ambient noise sources. Correction for time-series length can be achieved accurately by dividing the empirical Green's function by the squared root-mean-squared (rms) amplitude of the trailing noise. These results provide strong justification for the ability to constrain seismic attenuation using ambient noise with only slight refinements to traditional data processing schemes. However, further study of the expected asymmetry in attenuation for waves approaching (incoming) or receding from (outgoing) a central station is needed prior to estimation of local variations in attenuation.

1. Introduction

Surface wave tomography based on ambient noise cross-correlations is now commonly applied to constrain the elastic structure of the shallow earth (e.g. Shapiro et al. 2005; Yao et al. 2006; Lin et al. 2007; Yang et al. 2008; Moschetti et al. 2010; Lin et al. 2011). Studies of attenuation or anelasticity have been much more rare because of a relative lack of confidence in the interpretation of the amplitude content of ambient noise.

Tomographic studies based on ambient noise have focused nearly exclusively on the phase content of ambient noise cross-correlations partly because of uncertainty in the physical characteristics of ambient noise generation but also because ambient noise data processing procedures typically normalize amplitudes in a number of ways. Traditional data processing procedures (e.g., Bensen et al. 2007) such as temporal normalization (e.g., sign bit normalization, running mean normalization, etc) and spectral whitening are designed to suppress bias caused by earthquake signals and broaden the period range of the dispersion measurements. These procedures come with the cost of altering the amplitude content of the noise records and perhaps even degrading amplitude information irretrievably. This is exacerbated when seismic records have different time series lengths and in light of the strong azimuthal dependence and seasonal variability of ambient noise generation.

Recently, Cupillard and Capdeville (2009) presented numerical experiments that demonstrated that surface wave attenuation can be retrieved from one-bit noise

correlations as long as there is a uniform distribution of noise sources on the surface of the Earth. Observational studies of ground motion (Prieto & Beroza 2008) and attenuation (Prieto et al. 2009; Lawrence & Prieto 2010), also present an optimistic picture of the ability to exploit measurements of the amplitude of ambient noise. This paper is motivated by these studies. In particular, the question considered here is: Using traditional ambient noise data processing procedures, can surface wave amplitudes obtained from ambient noise cross-correlations produce reliable constraints on seismic attenuation or must data processing procedures be fundamentally revised in order to retain amplitude information? A particular interest is to determine the minimal set of refinements in ambient noise data processing needed to yield useful attenuation measurements.

The application of ambient noise to infer seismic attenuation is complicated by the expectation that attenuation measurements will differ for incoming and outgoing waves relative to a central station (i.e., positive and negative components of the cross-correlations) if the noise sources are dominantly in the far-field (Tsai, 2011). Addressing this distinction is beyond the scope of this paper, but this issue will need to be explored when ambient noise measurements are used to determine the attenuation structure of the earth. Here, we consider only if the spatially averaged attenuation determined from the symmetric component (the average of the incoming and outgoing waves) of the ambient noise cross-correlations is consistent with attenuation measured using regional seismic events observed across the USArray Transportable.

2. Data & Results

Bensen et al. (2007) and Lin et al. (2008) describe procedures for processing ambient noise records that have been shown to produce robust, largely unbiased measurements of Rayleigh and Love wave phase velocities. These procedures encompass both temporal and spectral whitening, deconvolution of the instrument response, calculation of the cross-correlation typically over day-long time series, stacking typically over numerous days, and construction of the empirical Green's function from on the symmetric component of the cross-correlation. These procedures together define what we refer to as the "traditional method" of ambient noise data processing in which no attempt has been made to retain amplitude information in the empirical Green's functions. Here we consider how these procedures must be altered so that attenuation can be inferred reliably from the amplitude measurements performed on the empirical Green's functions. To address this question we use ambient noise cross-correlations obtained between October 2004 and April 2010 using all EarthScope USArray Transportable Array stations in the US.

First, with traditional ambient noise data processing, aspects of the amplitude field are definitely lost. Because the amplitudes are normalized during temporal normalization and spectral whitening, the amplitude of ambient noise empirical Green's functions is rendered unitless and absolute amplitude information is lost. In addition, the ambient noise wavefield is normalized individually at each station so that local structural amplification (e.g., by sedimentary basins) is also lost. However, it is possible that propagation dependent attenuation, which requires only meaningful relative amplitude measurements, may be estimated reliably. This is the reason this paper focuses on the ability to recover information about attenuation.

To recover reliable relative amplitude measurements and use them to constrain attenuation, the traditional data processing method must be modified in two ways. First, it is important to account for the total length of the ambient noise records that were cross-correlated. We do this by dividing the empirical Green's function by the squared root-mean-squared (rms) amplitude of the trailing noise. (Here, we use trailing noise at correlation lags times between 1500 and 2500 sec.) As [Figure 1a](#) shows, in this time window the squared rms amplitude increases linearly with the duration of the cross-correlation time series and can be used as proxy for time series length. This approach would be particularly useful when the actual time series length is either unknown or known poorly, for example, due to gaps within the noise time series that were not kept track of accurately. We refer to empirical Green's functions processed in this way as "length-corrected". The second refinement in ambient noise data processing is discussed below.

To illustrate the amplitude measurements and attenuation coefficients determined from ambient noise, we use empirical Green's functions obtained between TA stations in the western US with two center stations M12A and I23A in northeastern Nevada and eastern Wyoming, respectively. These stations are chosen because they are near two seismic events, which allows us to compare directly the attenuative decay based on the ambient noise and seismic event measurements. The two events are the magnitude 6.0 Wells, Nevada earthquake (EQ) that occurred on February 21, 2008 and a large mining blast (MB) in eastern Wyoming that took place on August 6, 2009.

We perform frequency-time-analysis (FTAN; Bensen et al. 2007) to measure amplitudes between 5 and 25 sec period for both the ambient noise empirical Green's functions and

waveforms following the two seismic events. **Figure 1b-e** presents the length-corrected amplitude measurements that satisfy selection criteria at 18 sec period for ambient noise with center station M12A and the Nevada earthquake and at 10 sec period for ambient noise with center station I23A and the Wyoming mining blast. Amplitude measurements are used only when the signal-to-noise ratio is greater than 8 and distance is greater than 100 km and 50 km for 18 and 10 sec period, respectively. These selection criteria are designed to remove potentially inaccurate amplitude measurements.

For an impulsive force that emits a wave that propagates in a homogeneous attenuative medium, the amplitude A and the distance r are related at each period as follows:

$$A(r) = \frac{1}{\sqrt{r}} e^{-\alpha r} \quad (1)$$

where $1/\sqrt{r}$ results from geometrical spreading and α is the attenuation decay constant. α is related to the attenuation quality factor Q by $\alpha = \pi f / UQ$, where U is the group velocity and f is the wave frequency (e.g. Prieto et al. 2009). To test how well eq. (1) explains amplitude measurements obtained from the empirical Green's functions and whether α can be reliably constrained, **Figure 2a-b** presents the log of the length-corrected amplitude A_i corrected for geometrical spreading, $\log(A_i \sqrt{r_i})$, as a function of distance, r_i . The length-normalized amplitude measurements are taken from **Figure 1b-c** where i is the index for empirical Green's functions.

A clear distance trend is observed in **Figure 2a-b**, although scattering is significant. Measurements taken at similar azimuths, however, are much less scattered (red symbols in **Figure 2a-b**). As a preliminary constraint on the decay constant, measurements within

each 100 km bin are combined to estimate the mean and the standard deviation of the mean (blue bars in [Figure 2a-b](#)) and then fit with a straight line. The resulting slope and intercept are the best fitting decay constant and log corrected amplitude at zero distance. Distance bins with fewer than 20 amplitude measurements are discarded.

Most of the scatter about the linear trend seen in [Figure 2a-b](#) is caused by the azimuthal dependence of the strength of the incoming ambient noise energy, as seen clearly in the ambient noise amplitude measurements presented in [Figure 1b-c](#). Define the “amplitude factor” as ratio between the observed amplitude and the fit lines in [Figure 2](#). [Figure 3a-b](#) shows that the amplitude factor for ambient noise depends strongly on azimuth. We calculate the weighted average and the standard deviation of all the amplitude factors within each 8° azimuthal window where a Gaussian weight with 2° half width is used. Amplitude factors that deviate more than 1.5 standard deviations from the average are considered as outliers and discarded. Note that an approximate 180° azimuthal periodicity is observed for the amplitude factor shown in [Figure 3a-b](#), which is caused by the use of the symmetric component of the cross-correlations in constructing the empirical Green’s functions.

These observations lead to the second modification to the traditional ambient noise data processing procedure. To remove the effect of the azimuthal variations on the decay constant, we divide the amplitude measurements obtained on the length-corrected empirical Green’s functions by their corresponding azimuthally dependent average amplitude factor. We refer to the empirical Green’s function processed in this way as “azimuth corrected”.

Figure 4 presents the relationship between the length and azimuth corrected amplitude measurements versus distance. Compared to Figure 2a-b, a significant reduction in scattering is observed (Figure 4a-b). Following the same approach, the decay constant is re-estimated but with much lower uncertainty. The uncertainties with center stations M12A and I23A are now 2.4% and 5.8%, respectively, compared to 8.8% and 10.1% shown in Figure 2.

To determine whether the spatially averaged decay constants estimated from ambient noise are consistent with the measurements from the seismic events, Figure 4a-b presents amplitude measurements versus distance. The seismic events measurements are subjected to the same selection criteria as the ambient noise measurements and have also been azimuth-corrected to account for the source radiation pattern. In Figure 4c, we also present the result for central station M12A and the Wells, Nevada earthquake at 10 sec period. The Wyoming mining blast does not have good signals at 18 sec period and this result is not presented. In all three cases shown in Figure 4, the decay constants estimated from ambient noise and the seismic events are consistent, with differences around 6%, 4%, and 12% (or 1.4σ , 0.6σ , and 2.1σ where σ is the expected uncertainty for the difference) for Figure 4a, 4b, and 4c respectively.

The decay constants we observed are slightly smaller than the constants presented by Prieto et al. (2009) in southern California probably due to thicker sediments in southern California. The decay constants that we estimate here are averages over large regions surrounding the center station or seismic event where amplitude measurements are obtained. The $\sim 1 \times 10^{-3} \text{ km}^{-1}$ decay constant ($Q \sim 100$) at 10 sec observed with ambient noise for the center station M12A and the Wells, Nevada earthquake, is about two times

larger than the $\sim 4 \times 10^{-4} \text{ km}^{-1}$ decay constant ($Q \sim 200$) observed with ambient noise for the center station I23A and the Wyoming mining blast. This difference may reflect a warmer and perhaps weaker crust in northern Nevada and the Great Basin compared to eastern Wyoming and the Great Plains. While the mining blast does not provide good measurements at 18 sec period, the analysis at 18 sec period for ambient noise with central station I23A in Wyoming gives a decay constant of $\sim 3 \times 10^{-4} \text{ km}^{-1}$ ($Q \sim 200$), which is again roughly half of the decay constant ($\sim 6 \times 10^{-4} \text{ km}^{-1}$; $Q \sim 100$) observed for ambient noise with center station M12A and the Wells earthquake in the western US.

3. Discussion

We demonstrate here that the spatially averaged attenuation observed with ambient noise and regional seismic event measurements observed with the USArray Transportable array are highly consistent. In particular, we show that traditional ambient noise data processing procedures (e.g., Bensen et al., 2007) can be retained as long as amplitudes are corrected for (1) the duration of the ambient noise cross-correlation (length normalized), (2) geometrical spreading, and (3) the azimuthal variation in the strength of ambient noise sources (azimuth normalized). Length correction can be achieved accurately by dividing the empirical Green's function by the squared root-mean-squared (rms) amplitude of the trailing noise. These results corroborate the earlier studies of Prieto & Beroza (2008) and Prieto et al. (2009) and provide strong justification for the ability to constrain the attenuation structure of the earth using ambient noise, with only slight refinements in traditional data processing schemes.

The ability to constrain attenuation based on ambient noise empirical Green's is perhaps somewhat surprising. The effect of data processing procedures such as temporal normalization and spectral whitening on amplitude measurements is not as variable from station to station as previous suspected. This apparently is because amplitude normalization effects average out statistically for the long time series used here. Recently, Prieto et al. (2009) suggested that fundamental modifications to traditional data processing procedures were needed to obtain reliable amplitude information. In particular, they argued quite reasonably that the use of a shorter time window (e.g., 2-hr instead of one day) for cross-correlation would effectively remove earthquake signals but also retain more accurate information about the amplitude of ambient noise. However, the procedure they advocate is actually quite similar in effect to the temporal normalization that is applied in traditional ambient noise data processing (e.g., Bensen et al., 2007), where the average absolute mean is computed in a 128 sec sliding time window (Lin et al. 2008) and the time-series is normalized by this value. In addition, application of coherency, as advocated by Prieto et al. (2009), is similar to the cross-correlation with the spectral whitening that we apply. However, our use of spectral whitening inhibits observation of local amplification, but this may actually benefit observation of attenuation.

Finally, in order to exploit the attenuation measurements derived from ambient noise to infer the spatial variations in attenuation structure, or perhaps even the anelastic structure, of the Earth will require investigating the asymmetry in attenuation expected between waves approaching (incoming) or receding from (outgoing) from a central station. This will be the subject of a future study.

Acknowledgements

The authors gratefully acknowledge valuable conversations with Victor Tsai. Instruments (data) used in this study were made available through EarthScope (www.earthscope.org; EAR-0323309), supported by the National Science Foundation. The facilities of the IRIS Data Management System, and specifically the IRIS Data Management Center, were used for access the waveform and metadata required in this study. The IRIS DMS is funded through the National Science Foundation and specifically the GEO Directorate through the Instrumentation and Facilities Program of the National Science Foundation under Cooperative Agreement EAR-0552316. This work has been supported by NSF grants EAR-0711526 and EAR-0844097.

References

1. Bensen, G.D., M.H. Ritzwoller, M.P. Barmin, A.L. Levshin, F. Lin, M.P. Moschetti, N.M. Shapiro, and Y. Yang (2007), Processing seismic ambient noise data to obtain reliable broad-band surface wave dispersion measurements, *Geophys. J. Int.*, 169, 1239-1260, doi: 10.1111/j.1365-246X.2007.03374.x.
2. Cupillard, P. & Capdeville, Y. (2010), On the amplitudes of surface waves obtained by noise correlation and the capability to recover the attenuation: a numerical approach, *Geophys. J. Int.*, 181, 1687–1700.
3. Lin, F., M.H. Ritzwoller, J. Townend, M. Savage, S. Bannister (2007), Ambient noise Rayleigh wave tomography of New Zealand, *Geophys. J. Int.*, 18 pages, doi:10.1111/j.1365-246X.2007.03414.x.
4. Lin, F.-C., Moschetti, M. P., & Ritzwoller, M. H. (2008), Surface wave tomography

- of the western United States from ambient seismic noise: Rayleigh and Love wave phase velocity maps, *Geophys. J. Int.*, 173.
5. Lin, F.C., M.H. Ritzwoller, Y. Yang, M.P. Moschetti, and M.J. Fouch (2011), Complex and variable crustal and uppermost mantle seismic anisotropy in the western United States, *Nature Geoscience*, Vol 4, Issue 1, 55-61.
 6. Moschetti, M.P., M.H. Ritzwoller, F.C. Lin, and Y. Yang (2010), Seismic evidence for widespread crustal deformation caused by extension in the western USA, *Nature*, 464, Number 7290, 885-889, 8 April.
 7. Lawrence, J. F., Prieto, G. A. (2010), Attenuation tomography of the western united states from ambient seismic noise, *J. Geophys. Res.*, submitted.
 8. Prieto, G. A. & Beroza, G. C. (2008), Earthquake ground motion prediction using the ambient seismic field, *Geophys. Res. Lett.*, 35, 1–5.
 9. Prieto, G. A., Lawrence, J. F., & Beroza, G. C. (2009), Anelastic earth structure from the coherency of the ambient seismic field, *J. Geophys. Res.*, 114, 1–15.
 10. Shapiro, N. M., Campillo, M., Stehly, L., & Ritzwoller, M. H. (2005), High resolution surface-wave tomography from ambient seismic noise, *Science*, 307, 1615–1618.
 11. Tsai, V. (2011), Understanding the amplitudes of noise correlation measurements, *Geophys. J. Int.*, submitted.
 12. Yao, H., van der Hilst, R. D., & de Hoop, M. V. (2006), Surface-wave array tomography in SE Tibet from ambient seismic noise and two-station analysis - I. phase velocity maps, *Geophys. J. Int.*, 166, 732–744.

Figure Captions

Figure 1. (a) A linear relationship between squared rms amplitude of the trailing noise and the number of days being cross-correlated is demonstrated with the TA station pairs A23A-I23A (red plus) and J23A-I23A (green cross). (b) Length-corrected ambient noise amplitude measurements for the 18 sec Rayleigh wave with TA station M12A (star) at the center. Triangles are station locations with valid amplitude measurement where measured amplitudes are color coded within the triangle and interpolated between stations using minimum surface curvature. Dashed lines bracket the 340° and 360° azimuthal window for measurements shown in Fig. 2a. (c) Same as (b) but for the 10 sec Rayleigh wave with I23A at the center. Dashed lines bracket the 300° and 310° azimuthal window for measurements shown in Fig. 2b. The locations of stations A23A and J23A used in (a) are also identified. (d)-(e) Same as (b)-(c) but for the seismic event measurements following the Wells Nevada earthquake (EQ) and the Wyoming mining blast (MB) whose locations are shown with stars.

Figure 2. (a) The amplitude of ambient noise (corrected for time-series length and geometrical spreading) is plotted versus distance at 18 sec period for the TA central station M12A in Nevada. The red points are for measurements within the azimuthal window identified in Fig. 1b. The blue bars present the mean and the standard deviation of the mean of the measurements within each 100 km distance bin. Only bins with more than 20 measurements are kept. The solid black line is the best fitting line through the

blue bars; slope and intercept with uncertainties are labeled. (b) Same as (a) but for similarly corrected ambient noise measurements at 10 sec period for central station I23A in Wyoming where the red symbols are from the azimuthal window identified in [Fig. 1c](#).

Figure 3. (a) The azimuthal dependence of the amplitude factor for ambient noise amplitude measurements with central station M18A at 18 sec period corrected for time series length and geometrical spreading. The green solid line is the weighted average amplitude factor. (b) Same as (a) but for central station I23A at 10 sec period.

Figure 4. (a) Red symbols: the amplitude of ambient noise corrected for geometrical spreading as well as the length and azimuth corrections plotted versus distance at 18 sec period for the central station M12A (Nevada). Violet symbols: azimuthally corrected amplitudes measured at 18 sec period following the Wells earthquake. The green/yellow bars represent the mean and the standard deviation of the mean of all measurements within each 100 km bin and the solid blue/dashed black lines are the best fit lines. The y-axis on the left and right are for ambient noise and seismic event measurements, respectively. (b) Same as (a) but for measurements at 10 sec period for ambient noise at central station I23A (red symbols) and the Wyoming mine blast (violet symbols). (c) Same as (a) but for 10 sec Rayleigh wave measurements. The slope and intercept with uncertainties for the fit lines are labeled (AN – ambient noise; MB – mining blast; EQ – earthquake).

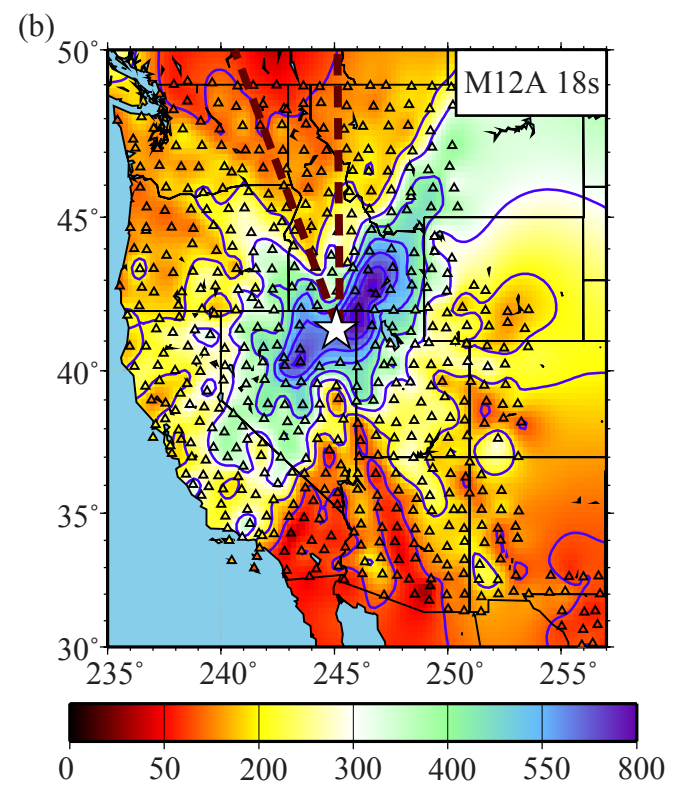
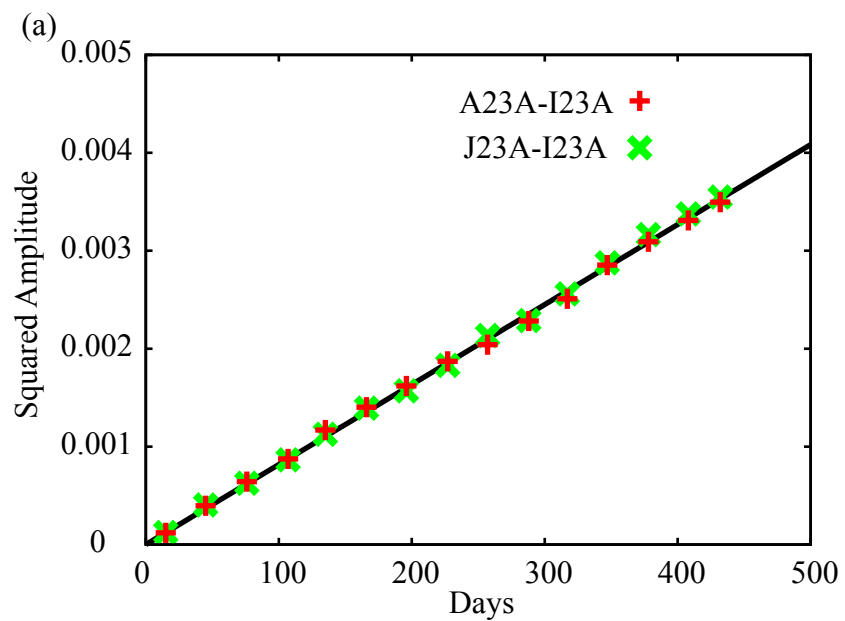
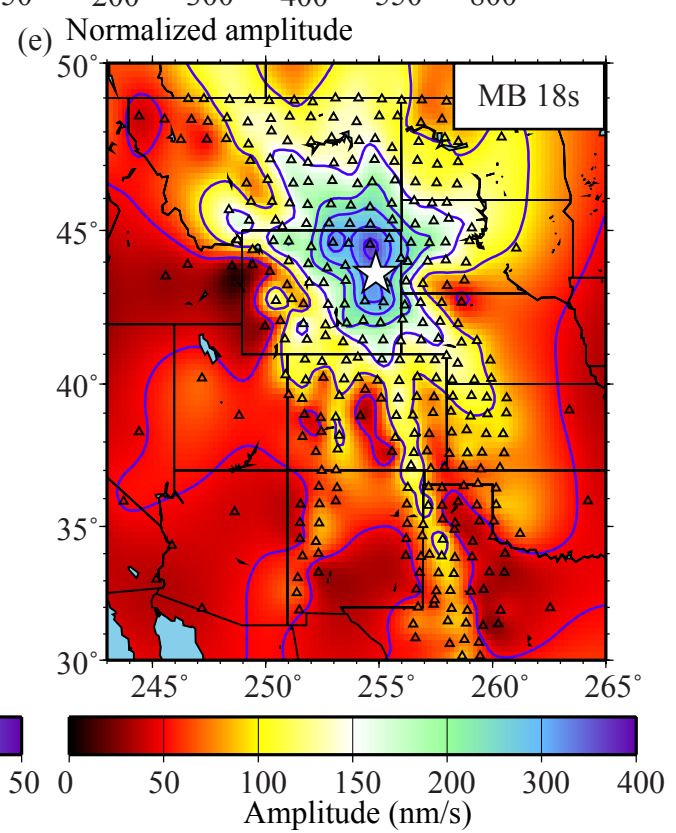
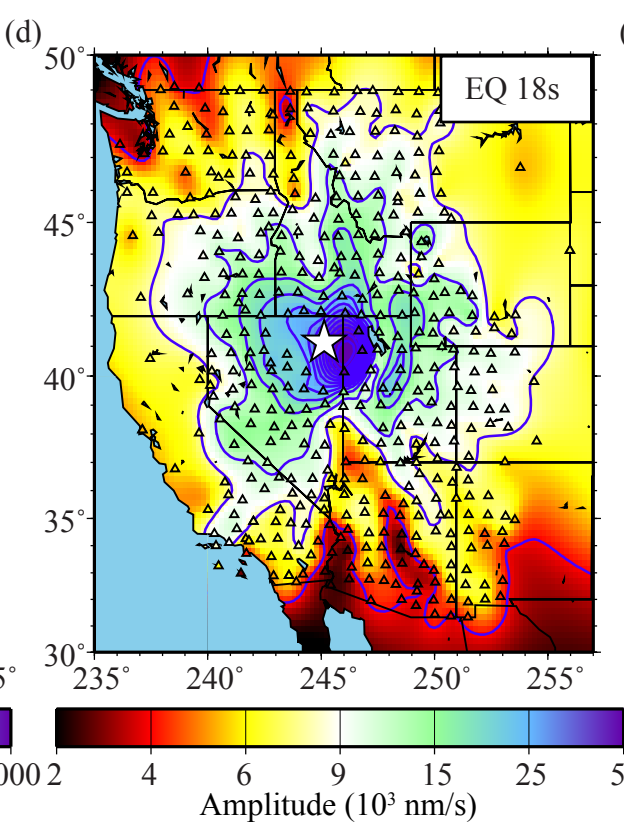
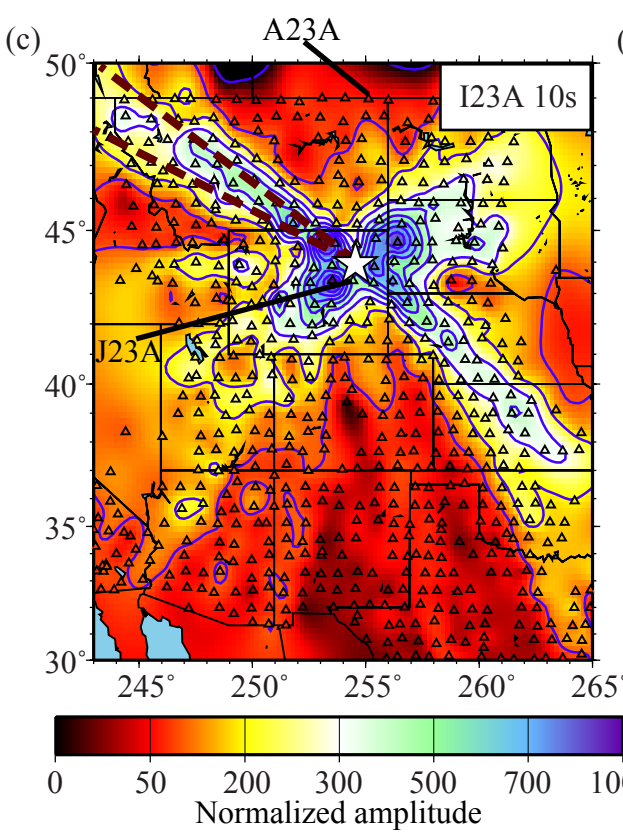


Figure 1



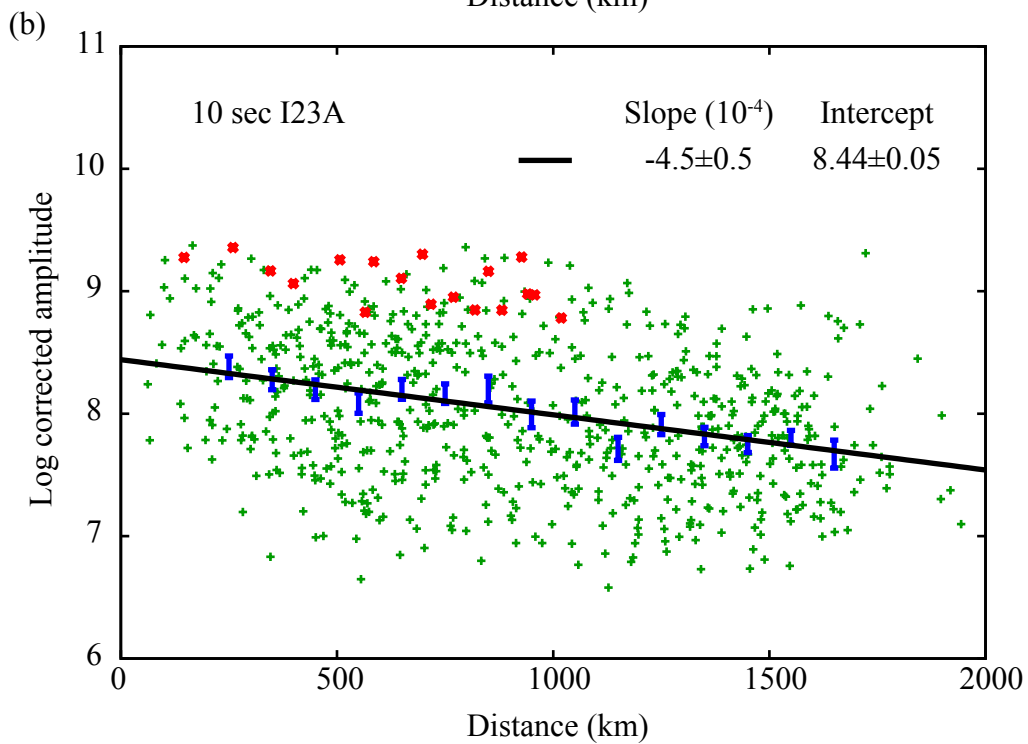
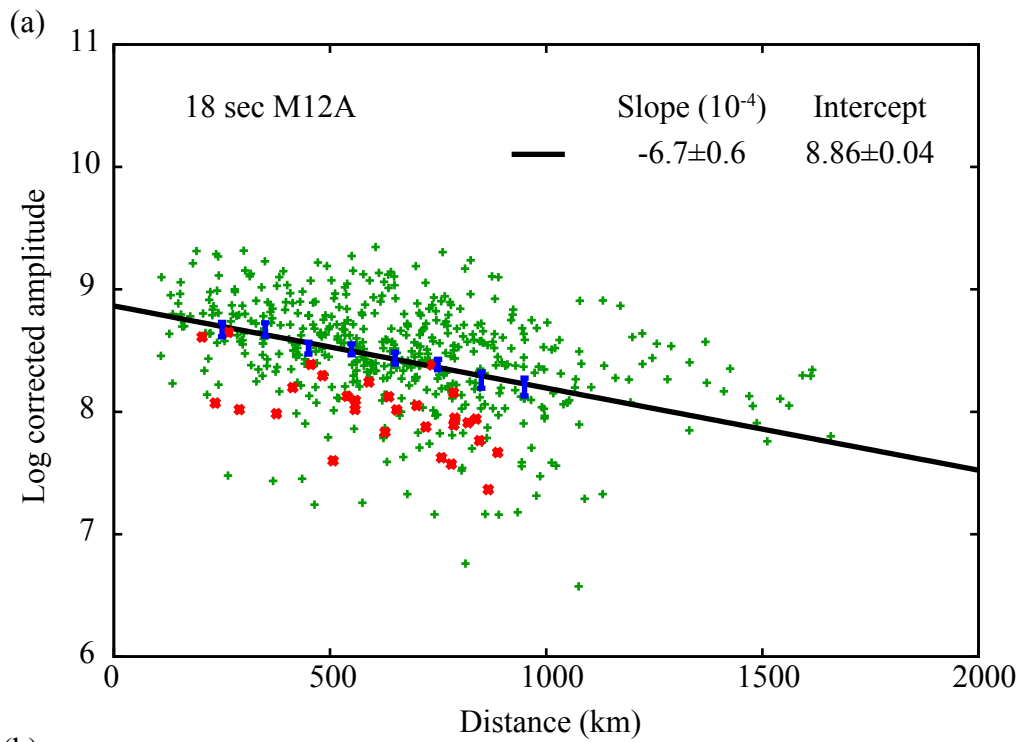


Figure 2

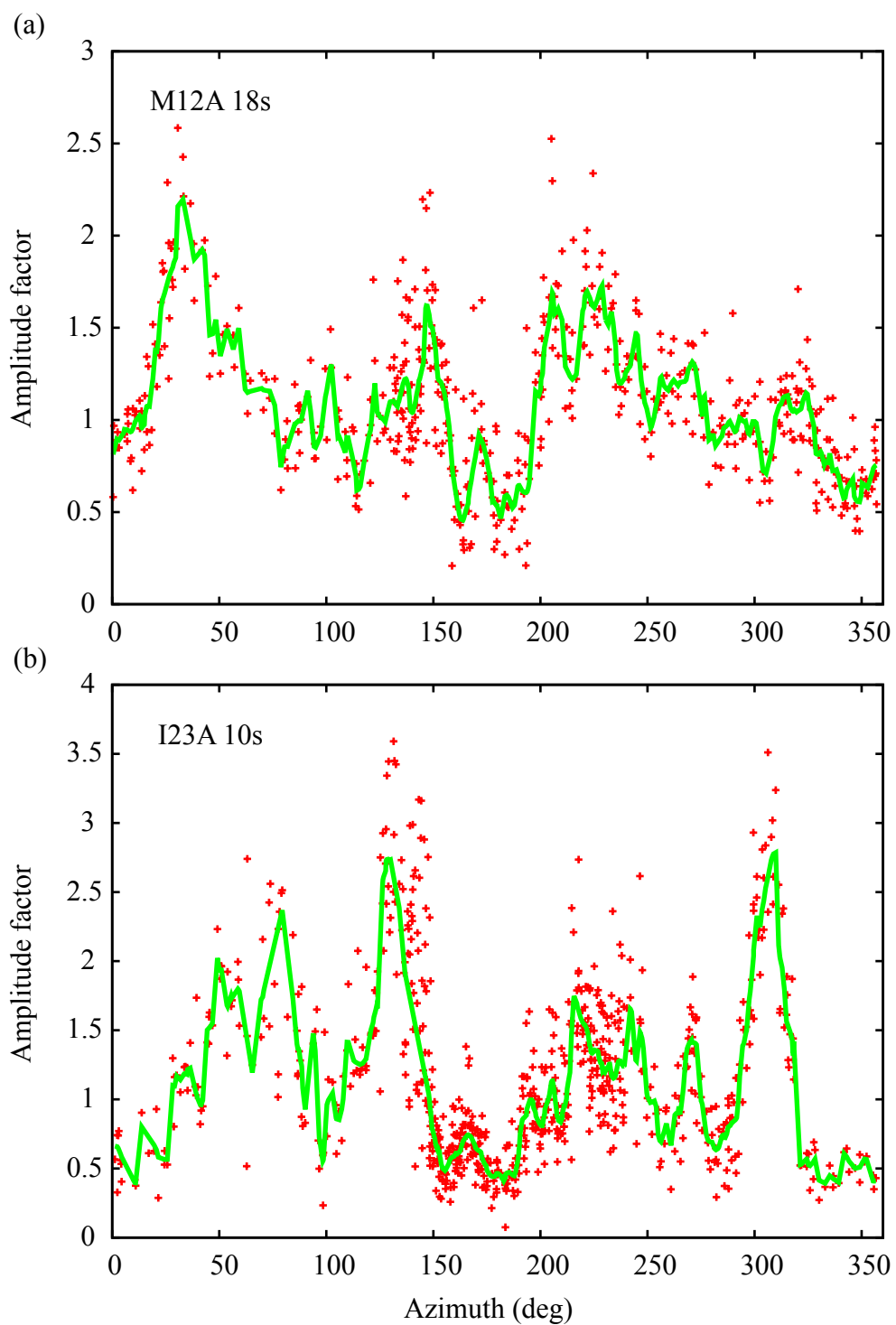


Figure 3

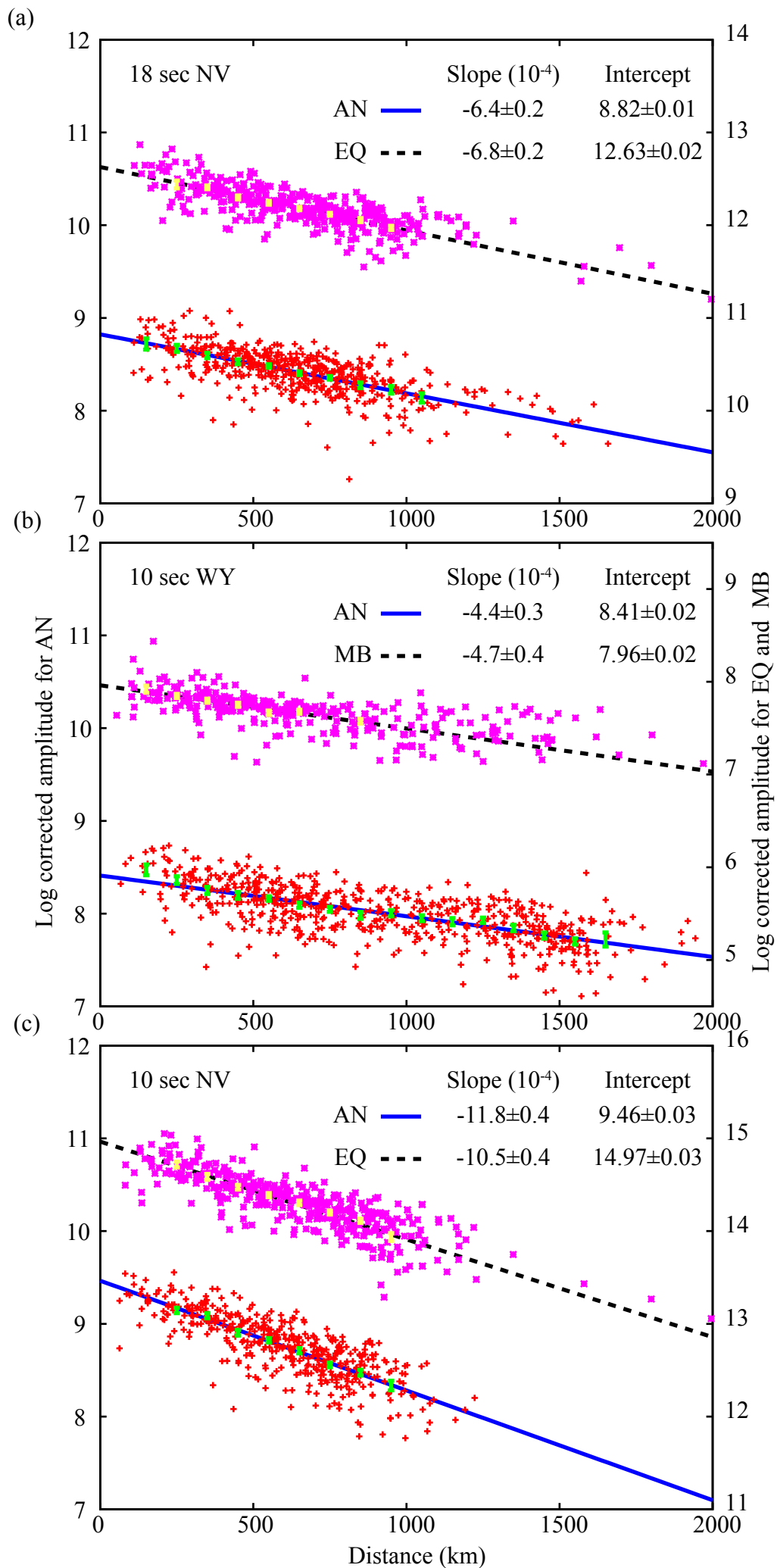


Figure 4